Electronic Supplementary Material (ESI) for Chemical Communications
This journal is © The Royal Society of Chemistry 2011

Supplementary Information

In vivo multimode Raman imaging reveals concerted molecular composition and distribution changes during yeast cell cycle

Chuan-Keng Huang,[a] Hiro-o Hamaguchi[a,b] and Shinsuke Shigeto*[a]

[a]*Department of Applied Chemistry and Institute of Molecular Science, National Chiao Tung University, Hsinchu, Taiwan.*
[b]*Department of Chemistry, School of Science, The University of Tokyo, Tokyo, Japan.*

*To whom correspondence should be addressed. E-mail: shigeto@mail.nctu.edu.tw.

Table of Contents

This journal is © The Royal Society of Chemistry 2011

Supplementary Results

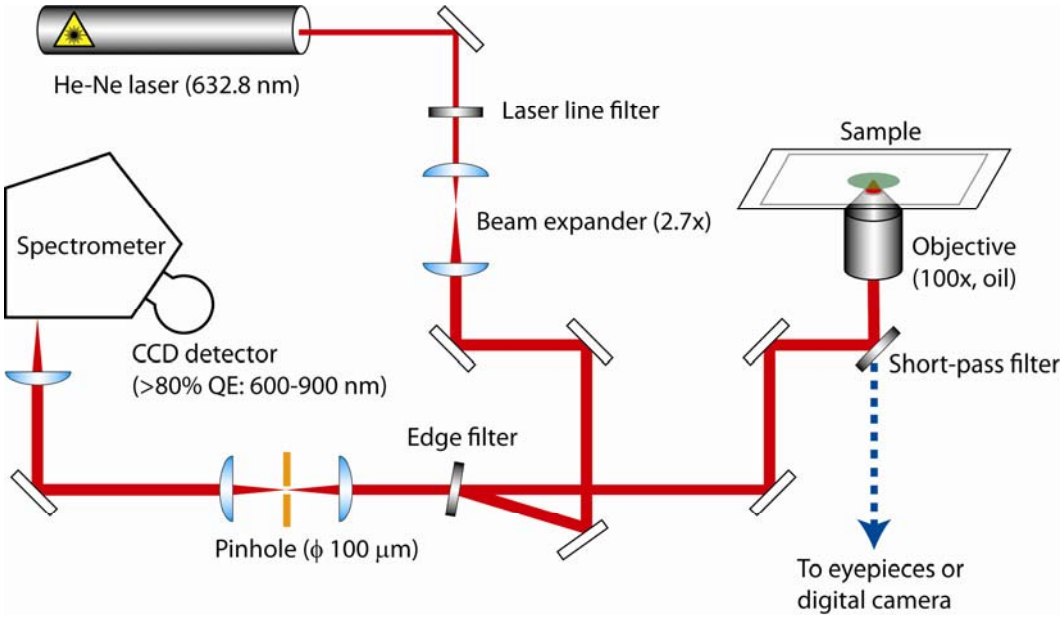

Fig. S1 Block diagram of our confocal Raman microspectrometer. Full details are given in the Supplementary Methods (see below). The apparatus consists of a He-Ne laser for Raman excitation, inverted microscope, imaging spectrometer and charge-coupled device (CCD) detector. To scan the sample and acquire Raman images, we combined a piezoelectric stage with the microscope stage.

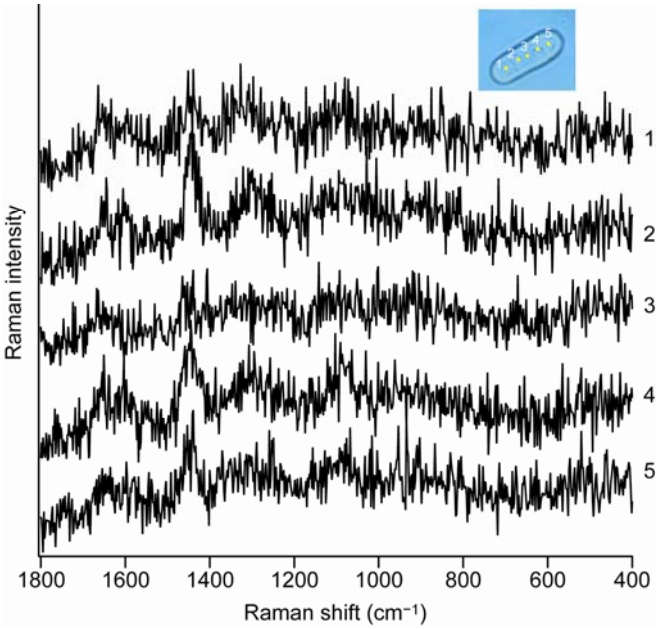

Fig. S2 Typical space-resolved Raman spectra of a single living *S. pombe* cell acquired with an exposure time of 1.5 s and laser power of 1 mW. The numbers 1–5 indicate the positions in the cell from which the Raman spectra were recorded. These Raman spectra are not treated with singular value decomposition (SVD) analysis but raw data. Without SVD analysis, the strongest band at 1440 cm^{-1} is only marginally seen and the other bands are completely buried under noise.

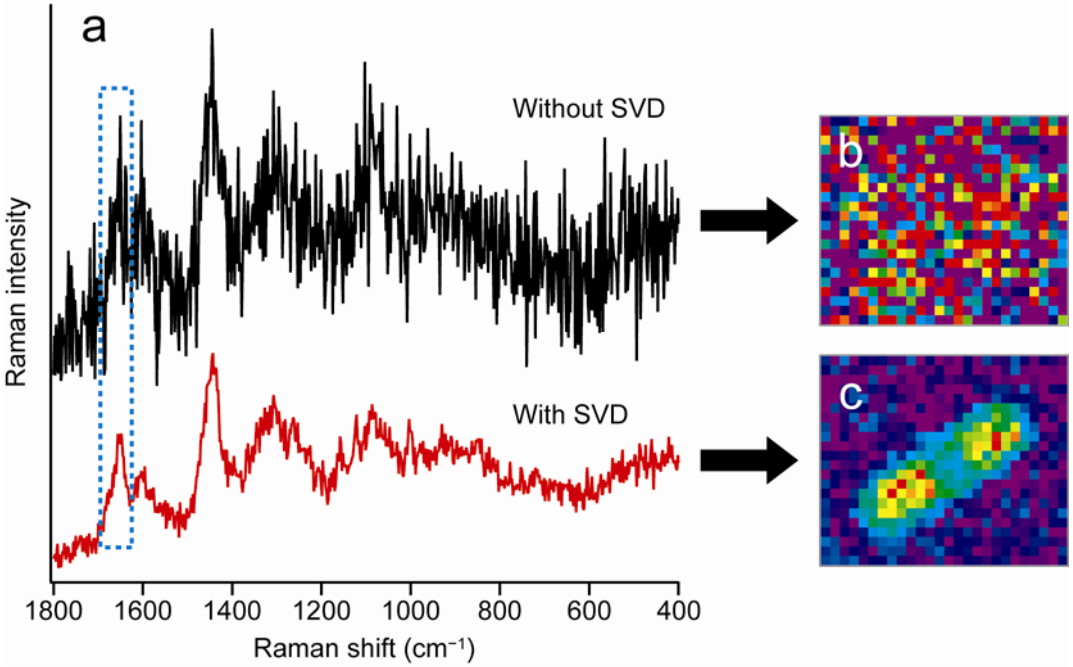

Fig. S3 (a) Comparison of raw and SVD-analyzed Raman spectra of a single *S. pombe* cell. The raw data recorded with an exposure time of 1.5 s were denoised by using SVD. It is clear that SVD considerably improved the signal-to-noise ratio without losing any characteristic features in the raw spectrum. (b,c) Raman images for the 1655 cm^{-1} band constructed from the raw and SVD-analyzed data, respectively. In b, even the shape of the cell is obscure, whereas in c, the heterogeneous intensity pattern inside the cell is clearly seen.

This journal is © The Royal Society of Chemistry 2011

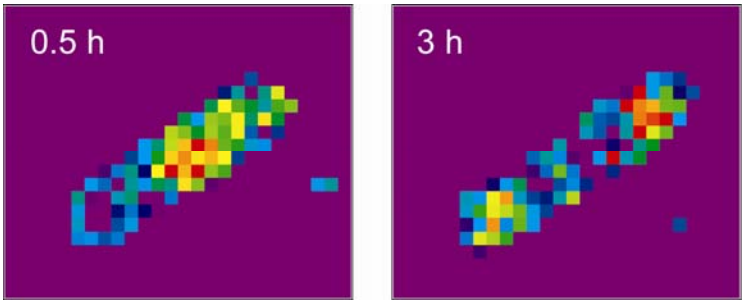

Fig. S4 Raman images of nucleic acids at the Raman shift of 783 cm^{-1} at 0.5 and 3 h. The Raman image at 0.5 h (left) shows that DNA exists at a high concentration at the centre of the *S. pombe* cell. Once a primary septum is formed and the cell is partitioned into two compartments prior to cytokinesis, DNA is also divided in two and localized around the centre of each compartment of the cell (3h, right). After 3 h, the intensity of the DNA band is too weak to produce meaningful Raman images.

This journal is © The Royal Society of Chemistry 2011

Table S1 Assignments of the nine Raman bands that are used to construct the Raman images in Figure 1.

Raman shift (cm^{-1})	**Assignment**
1655	C=C stretching of the unsaturated lipid chains Amide I mode of proteins
1602	Not yet assigned. 'Raman spectroscopic signature of life[1]'
1440	CH_2 scissoring and CH_3 degenerate deformation
1340	CH bending of the aliphatic chain of proteins
1301	In-plane CH_2 twisting
1260	C=C−H in-plane bending of the *cis* −CH=CH− linkage Amide III mode of proteins
1154	C−C and C−N stretching
1003	Ring breathing of the phenylalanine residues
852	'Tyrosine doublet' (Fermi resonance of a ring-breathing vibration and the overtone of an out-of-plane ring-bending vibration of the tyrosine residues)
783	Cytosine vibration and/or −O−P−O− symmetric stretching

This journal is © The Royal Society of Chemistry 2011

Supplementary Methods

Cell culture. *Schizosaccharomyces pombe*, a haploid yeast, was cultured on a YES plate containing yeast extract (5 g L^{-1}), glucose (30 g L^{-1}), agar (17 g L^{-1}), adenine, histidine, leucine, uracil and lysine (50 mg L^{-1} each). A single colony of the yeast was transferred into PM minimal medium with leucine and uracil[2] (75 mg L^{-1}) on a poly-D-lysine coated glass bottom dish (MatTek), where *S. pombe* cells were immobilized. An equivalent volume of YES medium was then added to supply more nutrition for better growth of the cells. Finally, the sample was housed in a laboratory-built humidity chamber mounted on a piezoelectric stage. This small chamber is designed so that it can fit into the aperture of the piezoelectric stage (~60 × 60 mm) and can accommodate a bottom dish. Water in the reservoir of the chamber prevents the medium from drying out during the 15-h Raman imaging experiment.

Confocal Raman microspectroscopy and imaging. We used a laboratory-built confocal Raman microspectrometer to perform Raman imaging experiments. The 632.8-nm output of a He-Ne laser (Thorlabs) was used as the Raman excitation light. The beam was magnified by a factor of ~2.7 to cover effectively the exit pupil of the objective used. The expanded beam was introduced to an inverted microscope (Nikon) by a pair of an edge filter (Semrock) and a hot mirror (KJ). We custom-made the microscope in collaboration with Nikon engineers by modifying a TE2000-U microscope. The beam was focused onto the sample by an oil-immersion objective (CFI Plan Fluor; 100×, NA = 1.3). To avoid possible detrimental effects of laser irradiation, the laser power was set to 1 mW at the sample point throughout the present study. The back-scattered light was collected by the same objective and guided along the same path as the incoming path but in the opposite direction. Rayleigh scattering was eliminated by the edge filter with high blocking of OD > 7, and only Stokes Raman scattering was transmitted. The Raman scattered light was then focused onto a 100-μm pinhole by a 150-mm lens and collimated by another 150-mm lens. This confocal arrangement achieved an axial resolution of 2.4 μm. The Raman scattered light was dispersed by an imaging spectrometer (HORIBA Scientific; iHR320) and detected by a back-illuminated, deep-depletion, liquid-N_2 cooled CCD detector (Princeton Instruments; Spec-10:100) with 100 × 1340 pixels operating at −120 ºC. A 600 grooves/mm grating was used to cover a wide spectral range (>2000 cm^{-1}) with an effective spectral resolution of 7 cm^{-1}. For bright-field observation, the sample was illuminated by a halogen lamp and optical micrographs were acquired by a digital camera (Nikon; DS-Ri1) mounted on the microscope.

We performed Raman imaging experiments by translating the sample horizontally with

a high-precision piezoelectric nanopositioning stage (PI; P-563.3CD), equipped on the microscope stage. The sample was translated with 0.5-μm steps in both X and Y directions. Because these steps were greater than the estimated lateral resolution (0.3 μm), they determined in effect the spatial resolution in this work. Spectral acquisition was synchronized with sample scanning by the computer program LabVIEW (National Instruments). At each position, the Raman spectrum was recorded with a 1.5-s exposure time. Therefore, approximately 18 min was needed to scan a target area of 23 × 32 pixels (= 11.5 × 16 μm^2). All measurements were done at 27 °C. This was to provide more favorable growth conditions to *S. pombe* cells compared with ambient temperature of 22–23 °C. The temperature of the medium in the humidity chamber was estimated to be 27(±0.5) °C.

The intensity of a Raman band was evaluated by calculating the area between the band contour and the baseline connecting the two edges of the band. The Raman intensities so obtained at each point were combined to construct two-dimensional maps of the Raman intensity distributions, namely, Raman images.

Spatial resolutions were 300 nm in the lateral (XY) direction and 2.4 μm in the axial (Z) direction. The lateral resolution was estimated by using the rise of the intensity profile of the Si first-order phonon band (520 cm^{-1}) at the infinitely sharp edge of a Si wafer. The axial resolution was confirmed by measuring the intensity rise of the 801 cm^{-1} band of cyclohexane at a cyclohexane–glass interface. We fit those intensity rises to Gaussian functions convolved with a step function.

Singular value decomposition analysis. To reduce noise in the Raman spectra recorded with an exposure time of 1.5 s, a numerical post-treatment was performed using singular value decomposition[3–5] (SVD). SVD is a mathematical technique that factorizes an arbitrary $m \times n$ matrix $\boldsymbol{A}$ into the product of three matrices as $\boldsymbol{A} = \boldsymbol{UWV}^{T}$. Here $\boldsymbol{U}$ is an $m \times n$ column-orthonormal matrix, $\boldsymbol{W}$ an $n \times n$ diagonal matrix of positive singular values, and $\boldsymbol{V}$ an $n \times n$ orthonormal matrix. In the present case, Raman spectra with 1340 pixels recorded at total 736 (= 23 × 32) different positions in the sample consisted of the matrix $\boldsymbol{A}$ (1340 × 736), whose column corresponded to the spectrum at a particular measurement point and row carried position information. $\boldsymbol{U}$ and $\boldsymbol{V}$ represented the spectral and positional matrices, respectively. Components of $\boldsymbol{U}$ and $\boldsymbol{V}$ that had small singular values were neglected, because their contributions to the original data $\boldsymbol{A}$ would be negligibly small. The matrix $\boldsymbol{A}$ was then reconstructed by using only the components of $\boldsymbol{U}$ and $\boldsymbol{V}$ associated with large singular values. The number of singular values retained in this reconstruction was typically less than 10. The

main criterion for determining how many components were taken into account was whether or not the spectral component of ***U*** corresponding to a particular singular value showed definite Raman features. The SVD was computed in Igor Pro (WaveMetrics) using LAPACK routines.

References

1. Y.-S. Huang, T. Karashima, M. Yamamoto, T. Ogura and H. Hamaguchi, *J. Raman Spectrosc.* 2004, **35**, 525–526.
2. S. Moreno, A. Klar and P. Nurse, *Methods Enzymol.* 1991, **194**, 795–823.
3. N. Uzunbajakava, A. Lenferink, Y. Kraan, E. Volokhina, G. Vrensen, J. Greve and C. Otto, *Biophys. J.* 2003, **84**, 3968–3981.
4. M. Okuno, H. Kano, P. Leproux, V. Couderc, J. P. R. Day, M. Bonn and H. Hamaguchi, *Angew. Chem. Int. Ed.* 2010, **49**, 6773–6777.
5. H. N. Noothalapati Venkata, N. Nomura and S. Shigeto, *J. Raman Spectrosc.* in press (DOI 10.1002/jrs.2952).